



Archaeointensity study of five Late Bronze Age fireplaces from Corent (Auvergne, France)

Gwenaël Hervé, Annick Chauvin, Pierre-Yves Milcent, Arthur Tramon

► To cite this version:

Gwenaël Hervé, Annick Chauvin, Pierre-Yves Milcent, Arthur Tramon. Archaeointensity study of five Late Bronze Age fireplaces from Corent (Auvergne, France). *Journal of Archaeological Science: Reports*, 2016, 7, pp.414-419. 10.1016/j.jasrep.2016.05.018 . insu-01322354

HAL Id: insu-01322354

<https://hal-insu.archives-ouvertes.fr/insu-01322354>

Submitted on 27 May 2016

HAL is a multi-disciplinary open access archive for the deposit and dissemination of scientific research documents, whether they are published or not. The documents may come from teaching and research institutions in France or abroad, or from public or private research centers.

L'archive ouverte pluridisciplinaire **HAL**, est destinée au dépôt et à la diffusion de documents scientifiques de niveau recherche, publiés ou non, émanant des établissements d'enseignement et de recherche français ou étrangers, des laboratoires publics ou privés.

Archaeointensity study of five Late Bronze Age fireplaces from Corent (Auvergne, France)

Gwenaël Hervé ^{1*}, Annick Chauvin ², Pierre-Yves Milcent ³, Arthur Tramon ³,

(1) Department für Geo- und Umweltwissenschaften, Ludwig-Maximilians Universität, Munich, Theresienstrasse 41, 80333 München, Germany.

(2) Géosciences-Rennes, UMR 6118, CNRS, Université Rennes 1, Campus de Beaulieu, 35042 Rennes cedex, France.

(3) TRACES, UMR 5608, CNRS, Université Toulouse – Jean Jaurès, Maison de la Recherche, 5 allée Antonio Machado, 31058 Toulouse Cedex 9, France.

* Corresponding author : gherve@geophysik.uni-muenchen.de

Abstract

Recent excavations at Corent (France) unearthed a vast Late Bronze Age settlement. The high density of fireplaces especially highlights it. The present study focuses on the archaeomagnetic study of five fireplaces. These ones were dated between 950 and 800 BC by cross-dating of metallic and ceramic artefacts and by radiocarbon. The main objective of our study is to increase the archaeointensity database in Western Europe at the beginning of the first millennium BC. The sampling was conducted on 64 fragments of baked clay and sherds from the fireplaces floor. The classical Thellier-Thellier protocol provides 48 successful archaeointensity results, yielding to five mean values between 58 and 69 μT at the site. Together with previously published results, our new data point out two successive maxima of the intensity of the geomagnetic field. The first maximum $\sim 70 \mu\text{T}$ in the ninth century BC and the second $\sim 90 \mu\text{T}$ in ~ 700 BC are separated by a $\sim 45\text{-}50 \mu\text{T}$ minimum at $\sim 800\text{-}750$ BC. The resulting fast variation of the field intensity will be very useful for archaeomagnetic dating purposes. As the direction of the geomagnetic field has also a strong variation during this period (Hervé *et al.*, 2013a), archaeomagnetism promises to be a powerful dating tool to recover the historical processes at the transition between the Bronze and Iron Ages in Western Europe.

Keywords

archaeomagnetism; archaeointensity; France; Late Bronze Age; Puy de Corent

1. Introduction

The number of archaeomagnetic intensity results considerably grew in Western Europe during the last few years (e.g. Genevey et al., 2009, 2013; Gómez-Paccard et al., 2008, 2012; Hervé et al., 2013b; Schnepf et al., 2009; Tema et al., 2013). Most of them cover the past 2500 years and only few have been published for older periods (Aidona et al., 2006; Gallet et al., 2009; Hervé et al., 2011; Hill et al., 2008; Kapper et al., 2015; Kovacheva et al., 2009). The latter highlight a fast secular variation in intensity, especially between 1000 and 500 BC that is at the Late Bronze Age and the Early Iron Age. This fast changing of intensity was also recovered in the Middle East (e.g. Ertepinar et al., 2012; Gallet and Le Goff, 2006; Gallet et al., 2015; Kovacheva et al., 2014; Shaar et al., 2011). A better constraint of the secular variation during this period in Western Europe will allow to better understand the geomagnetic field behaviour at the regional and global scale (Hong et al., 2013).

By the other hand, this fast secular variation lets also expect a great potential for the archaeomagnetic dating technique. A directional (inclination and declination) curve is already available for Western Europe (Hervé et al., 2013a). However, Western Europe intensity data for Late Bronze and Early Iron Age are still too few to build a precise and accurate regional secular variation curve. Adding the intensity to the direction will provide a more efficient chronological tool for archaeologists. The five new data from the Late Bronze Age settlement of Corent presented in this study are a new step to better recover the intensity secular variation in Western Europe and to improve the dating method for this period.

2. Archaeological context

The Puy de Corent is located on a plateau overlooking the Grande Limagne plain, 19 km away from Clermont-Ferrand in Auvergne (Latitude: 45.665°N; Longitude: 3.189°E). Since 2001, two teams of researchers have excavated this site, one from Université Lumière Lyon II conducted by Matthieu Poux and another one from Université Toulouse – Jean Jaurès conducted by Pierre-Yves Milcent. This location is very famous for its *oppidum* of the Late La Tène period, but is also characterized by earlier important agglomerations (Milcent *et al.*, 2014a and 2014b).

One of these important occupations of Puy de Corent's is dated at the end of the Bronze Age (from the end of the 11th to the end of 9th century BC), during which a vast and dense settlement developed on the lower part of the plateau and covered a minimum surface of 15 ha (Figure 1a). Its limits have not yet been reached and we have now some evidence that the site could be one of the first proto-urban settlements in Western Europe (Ledger *et al.*, 2015). Three successive phases of occupation and development of the agglomeration were recognized: "Bronze Final 2 récent" (~1050 – ~950 BC), "Bronze Final 3 ancien" (~950 – ~900 BC) and "Bronze Final 3 récent" (~900 – ~800 BC). These phases are determined by stratigraphy. They are dated by few radiocarbon dates and by comparison of the abundant ceramics and metallic artefacts with similar objects coming from accurately dated alpine lake's palafittes. The various occupation levels display a high density of fireplaces, also dated by their relative positions in the stratigraphic sequence and according to their close relationships with the ceramic and metallic material. Radiocarbon dating (Lyon-11289, 2785±35 BP) of the occupancy level numbered [20450] related to the fireplace FY20462, assigned to "Bronze Final 3 ancien" by ceramics, confirms the archaeological dating ([950; 900] BC) with the dating interval

[1012; 839] BC at 95 per cent of confidence and [979; 899] BC at 68 per cent of confidence.

The 64 fireplaces of the Late Bronze Age (1 per 50 m² in average) discovered since 2001 display, whatever their phase, some recurrent features in their shape and their construction type. Most of the time, fireplaces are built on simple or mixed raft foundation of small pebbles, basalt blocks, re-used fragments of stone macro-equipment (grindstones and granite thumb-wheels) or ceramic sherds (Figure 1b-c). They support screeds with thickness generally varying between 1 and 3 cm made of mixed clay and sand. The best-preserved fireplaces are either circular or rectangular with round angles, and measure between 1.00 and 1.60 m of diameter for the first ones, and 0.95 m x 0.70 m for the latter. Repeatedly, we observed, under the raft foundation and in the center of the fireplace, a little *locus* with a depth of 5 to 10 cm and with a diameter varying from 18 to 28 cm. Although they seemed sealed by the fireplace, some *loci* sheltered another deliberate deposition. The deposition are composed of bone, bronze objects (pin, ring, metal droplet) and even exceptionally a fig seed, whose the growing was limited to the Mediterranean regions at the Late Bronze Age. Positioning exactly the fireplaces in relation to the constructions on standing posts of the site remains difficult: while some were clearly inside the buildings, others seem to have been outside.

3. Archaeomagnetic analyses

3.1 Sampling

We sampled five fireplaces. The best-preserved fireplaces FY20462 and FY22783 (Figure 1b) were sampled *in-situ* using plaster cap method. Respectively 9 and 13 blocks

of baked clay were surrounded with plaster, levelled horizontally using a bubble and oriented using a magnetic compass. In the laboratory of Rennes, the baked clay fragments were prepared in 8 cm³ cubic specimen after consolidation using sodium silicate. In the case of the disturbed fireplaces FY22705, FY22798 and FY22842 (Figure 1c), we collected without orientation between 12 and 16 baked clay fragments and pottery sherds per structure. Those and the pottery sherds of the fireplaces FY20462 and FY22783 were divided in ~1 cm³ chips with the same orientation. The cutting reference was a flat side of the fragment or the sherd, which corresponded or was parallel to the surface of the fireplace. This would help to identify the component of remanent magnetization acquired *in situ*. Each chip was then packed into cylindrical quartz holder filled by quartz wool.

3.2 Rock magnetism

To investigate the ferromagnetic mineralogy, thermomagnetic curves were measured on small chips of 34 samples using a KLY3-CS3 susceptibility meter with a fitted furnace. The variation of the susceptibility was measured during heating to 400 and 600°C and during the subsequent cooling. In all baked clay fragments and pottery sherds, thermomagnetic curves reveal a dominant ferromagnetic phase with Curie temperatures between 550 and 580°C identified as titanium-poor titanomagnetite (Figure 2a-b). All heating-cooling cycles (up to 600°C) of pottery sherds are reversible (Figure 2b). On some fragments of baked clay the slight irreversibility suggests mineralogical evolutions at high temperature (Figure 2a). None samples were nevertheless rejected for archaeointensity experiments, because all cycles up to 400°C were fully reversible. Isothermal remanent magnetization (IRM) acquisition curves were

acquired on 21 specimens using an ASC impulse magnetizer. Saturation occurred at low magnetic fields (~300 mT), indicating the lack of any high-coercivity ferromagnetic phase (Figure 2c).

3.3 Thermal demagnetization

Prior to the archaeointensity experiment, one specimen per sample was thermally demagnetized in a Magnetic Measurement Thermal Demagnetizer (MMTD) oven, in order to identify the component of thermoremanent magnetization (TRM) acquired *in situ*. Sample's positions in the field suggest that the expected TRM should have an inclination of circa $\pm 60-70^\circ$, as based on the data from the neighbour and contemporaneous site of Lignat (Gallet et al., 2002; Moutmir, 1995).

Almost all (50/54) fragments of backed clay from the upper layer of the fireplaces carry a single TRM component with the expected inclination. Three pottery sherds carry two clear components of magnetization. The low-temperature component between 100 and 400-500°C has a $\sim 60-70^\circ$ inclination and was therefore acquired *in situ*. Directions of the high-temperature component are totally dispersed and they are probably associated to the initial firing of the pottery. As these three sherds were found below the baked clay layer, they reached a lower temperature during the last heating of the fireplace and therefore they carry two components of magnetization. Six pottery sherds (three from FY22798 and three from FY22842) and four baked clay samples (from FY 22798) have a multiple component magnetization, none of them close to the expected inclination. We did not perform archaeointensity experiment on these ten samples.

Oriented block samples from FY20462 and FY22783 carry a TRM with an easterly declination and an inclination in the range of the expected values for the Late Bronze Age (Hervé *et al.*, 2013a) (Figure 3). However the scatter between directions indicates slight displacements of the baked clay fragments since the last high-temperature heating and prevents the calculation of a mean direction of magnetization.

3.4 Archaeointensity study

Archaeointensity experiments were performed using the classical Thellier-Thellier method (Thellier and Thellier, 1959) with partial thermoremanent magnetization (pTRM) checks on 56 specimens (50 baked clay fragments and 6 pottery sherds). At each temperature step, specimens were heated and cooled twice, first in a laboratory field $+F_{lab}$ and secondly in the opposite field $-F_{lab}$ of 60 μT . The protocol was performed using 13 temperature steps up to 570 or 580°C in a Pyrox amagnetic oven. All remanent magnetization were measured with a 2G cryogenic magnetometer. The anisotropy of TRM was determined at 510 or 540°C using 6 successive heating and one stability check (Chauvin *et al.*, 2000). The cooling rate effect on TRM intensity was also corrected at 535 or 555°C using the procedure in four heating steps of Gómez-Paccard *et al.* (2006). The slow cooling rate was fixed to 8 hours.

We used the following criteria to select the specimens for the mean archaeointensity calculation: NRM fraction factor higher than 0.5, maximum angular deviation Mad lower than 5°, deviation angle $Dang$ lower than 5° and ratio of the standard error of the slope to the absolute value of the slope β lower than 0.05. A pTRM-check was said positive if its difference with the original pTRM was lower than 10%. Samples showing a concave-

up NRM-TRM diagram indicating some mineralogical changes during heating were rejected from the analysis (Figure 4a). All the accepted specimens have a linear NRM-TRM diagram (Figure 4b). In the case of pottery sherds, the archaeointensity was computed using the secondary component of magnetization after correction of the NRM-TRM diagram (Hervé et al., 2013b, Figure 4c). The selection procedure yields an acceptance rate of 86% (Supplementary material).

The archaeointensity values were corrected for TRM anisotropy if the alteration factor inferred from the stability check was lower than 10%. The anisotropy degree varied from 3 to 27%. The cooling rate correction was applied only when the absolute value of the correction factor was higher than the alteration factor (Gómez-Paccard et al., 2006). Otherwise, that is for ten specimens, the cooling rate correction was not accounted for. The correction factor was usually lower than 6%, except for specimens from FY20462 with values between 10 and 15%. The mean archaeointensity per fireplace was computed using the weighting method of Prévot et al. (1985) (Table 1). The five mean values agree well with each other.

4. Discussion

Our new mean archaeointensities were relocated to Paris using the Virtual Axial Dipole Moment (VADM) correction. On Figure 5, they are compared to published Western European data for Late Bronze and Iron Ages. These data include the selected data set described in Hervé et al., (2013b) completed by new Swiss data (in grey on Figure 5, Kapper et al., 2015). Given the small number of published results, the five fireplaces of Corent represent a significant step to recover the secular variation of the geomagnetic

199 field intensity between 1500 and 600 BC. The large range of archaeointensities (~50-
200 90 μ T) between 1000 and 600 BC points out high and fast variations of the geomagnetic
201 field strength.

202 An increase of the field intensity is observed during the tenth century BC up to ~65-70
203 μ T, followed by a possible decrease during the ninth century with values close to 45 μ T
204 at ~800-750 BC. After that, the intensity would increase up to ~90 μ T in ~700-600 BC, as
205 supported by Gallet et al. (2009), Hervé et al. (2011) and Hill et al. (2008) data.

206 From ~800 to ~700-600 BC, the secular variation rate would have been around ~3
207 μ T/decade. This rate is higher than the typical one (1 μ T/decade) observed over the last
208 two millennia in Western Europe (Genevey et al., 2013) but is similar to the rate during
209 the early Middle Age (Gómez-Paccard et al., 2012). The sharp secular variation at the
210 beginning of the Early Iron Age may be recorded in the Swiss mean data with an unusual
211 standard deviation of 15.5 μ T (Kapper et al., 2015, grey triangle data on Figure 5). This
212 average archaeointensity was computed from two pottery sherds coming from the same
213 archaeological layer. They provide archaeointensities of 45 and 75 μ T. We suggest that
214 these potteries were magnetized at slightly different times during a period of fast
215 changes of the field intensity.

216 The Corent data do not record the geomagnetic spikes (short-lived high field anomalies),
217 highlighted in the Levantine area during the ninth century BC (Ben-Yosef et al., 2009;
218 Shaar et al., 2011). Other new reference data are needed to investigate the presence of
219 such events in Western Europe and to better estimate the secular variation rate during
220 the Late Bronze Age.

Finally, our new data are compared to the prediction at Paris of the geomagnetic model SHA.DIF.14k that is valid in the Northern hemisphere (Figure 5)(Pavón-Carrasco et al., 2014a). This model is developed by inversion of archaeomagnetic and volcanic results using spherical harmonic analysis in space and penalised cubic B-splines in time. For the 1500-500 BC time period the data set used to build the model includes a large amount of results obtained on Eastern Europe sites. All the data in black on Figure 5 are also used to build the SHA.DIF.14k model but not the more recently published Swiss data in grey (Kapper et al., 2015). The SHA.DIF.14k model's prediction does not fit well most of the data between 1000 and 500 BC. Maxima of intensity are observed but with shifts in time and amplitude compared to Western Europe archaeointensity results. The archaeointensity values obtained at Corent are higher than the model's prediction and differ up to 15 μ T. Inhomogeneous quality of the archaeointensities and inhomogeneous geographical distribution of sites in the global database probably explains these inconsistencies (Pavón-Carrasco et al., 2014b). Finally this comparison indicates that reliable intensity data are still needed in order to better constrain global models of the past geomagnetic field.

5. Conclusion

The study of fireplaces from the archaeological site Puy de Corent provides five new high quality archaeointensities at the Late Bronze Age in Western Europe. This represents a new step to increase the amount of reliable data set and to build a reference curve of the secular variation of the geomagnetic field intensity. The large and fast secular variation at the Late Bronze Age and the Early Iron Age lets expect that this reference curve will give precise archaeomagnetic dating both for in place and displaced

objects. Together with directional data of the geomagnetic field, which also shows large variations, archaeomagnetic dating technique will provide a very valuable alternative to radiocarbon, especially problematic during this period due to plateau effects. Archaeomagnetism will efficiently contribute to the refinement of our knowledge of the evolutions of the societies in Western Europe at the transition from the Bronze Age to the Iron Age.

Acknowledgements

GH thanks the Deutsches Forschung Gemeinschaft for funding (project HE7343/1-1). Philippe Cullerier is kindly acknowledged for his help in sample's preparation and Thellier-Thellier measurements. We thank an anonymous reviewer for his/her insightful review.

References

- Aidona, E., Scholger, R., Mauritsch, H.J., Schnepf, E., Klemm, S., 2006. Spatial distribution of archaeomagnetic vectors within archaeological samples from Eisenerz (Austria). *Geophys. J. Int.* 166, 46–58. doi:10.1111/j.1365-246X.2006.02944.x
- Ben-Yosef, E., Tauxe, L., Levy, T.E., Shaar, R., Ron, H., Najjar, M., 2009. Geomagnetic intensity spike recorded in high resolution slag deposit in Southern Jordan. *Earth Planet. Sci. Lett.* 287, 529–539. doi:10.1016/j.epsl.2009.09.001

265 Chauvin, A., Garcia, Y., Lanos, P., Laubenheimer, F., 2000. Paleointensity of the
 266 geomagnetic field recovered on archaeomagnetic sites from France. *Phys. Earth Planet.*
 267 *Inter.* 120, 111–136.

268 Ertepinar, P., Langereis, C.G., Biggin, A.J., Frangipane, M., Matney, T., Ökse, T., Engin, A.,
 269 2012. Archaeomagnetic study of five mounds from Upper Mesopotamia between 2500
 270 and 700 BCE: Further evidence for an extremely strong geomagnetic field ca. 3000 years
 271 ago. *Earth Planet. Sci. Lett.* 357-358, 84–98. doi:10.1016/j.epsl.2012.08.039

272 Gallet, Y., Le Goff, M., 2006. High-temperature archeointensity measurements from
 273 Mesopotamia. *Earth Planet. Sci. Lett.* 241, 159–173. doi:10.1016/j.epsl.2005.09.058

274 Gallet, Y., Genevey, A., Le Goff, M., 2002. Three millennia of directional variation of the
 275 Earth's magnetic field in western Europe as revealed by archeological artefacts. *Phys.*
 276 *Earth Planet. Inter.* 131, 81–89. doi:10.1016/S0031-9201(02)00030-4

277 Gallet, Y., Genevey, A., Le Goff, M., Warmé, N., Gran-Aymerich, J., Lefèvre, A., 2009. On
 278 the use of archeology in geomagnetism, and vice-versa: Recent developments in
 279 archeomagnetism. *Comptes Rendus Phys.* 10, 630–648. doi:10.1016/j.crhy.2009.08.005

280 Gallet, Y., Molist, M., Genevey, A., Clop, X., Thébault, E., Gómez, A., Le, M., Robert, B.,
 281 Nachasova, I., 2015. New Late Neolithic (c . 7000 – 5000 BC) archeointensity data from
 282 Syria. Reconstructing 9000 years of archeomagnetic field intensity variations in the
 283 Middle East. *Phys. Earth Planet. Inter.* 238, 89–103. doi:10.1016/j.pepi.2014.11.003

284 Genevey, A., Gallet, Y., Rosen, J., Le Goff, M., 2009. Evidence for rapid geomagnetic field
 285 intensity variations in Western Europe over the past 800 years from new French

286 archeointensity data. *Earth Planet. Sci. Lett.* 284, 132–143.
 287 doi:10.1016/j.epsl.2009.04.024

288 Genevey, A., Gallet, Y., Thébault, E., Jesset, S., Le Goff, M., 2013. Geomagnetic field
 289 intensity variations in Western Europe over the past 1100 years. *Geochemistry,*
 290 *Geophys. Geosystems* 14, 2858–2872. doi:10.1002/ggge.20165

291 Gómez-Paccard, M., Chauvin, A., Lanos, P., Thiriot, J., Jiménez-Castillo, P., 2006.
 292 Archeomagnetic study of seven contemporaneous kilns from Murcia (Spain). *Phys.*
 293 *Earth Planet. Inter.* 157, 16–32. doi:10.1016/j.pepi.2006.03.001

294 Gómez-Paccard, M., Chauvin, A., Lanos, P., Thiriot, J., 2008. New archeointensity data from
 295 Spain and the geomagnetic dipole moment in western Europe over the past 2000 years. *J.*
 296 *Geophys. Res.* 113, B09103. doi:10.1029/2008JB005582

297 Gómez-Paccard, M., Chauvin, A., Lanos, P., Dufresne, P., Kovacheva, M., Hill, M.J.,
 298 Beamud, E., Blain, S., Bouvier, A., Guibert, P., 2012. Improving our knowledge of rapid
 299 geomagnetic field intensity changes observed in Europe between 200 and 1400 AD.
 300 *Earth Planet. Sci. Lett.* 355–356, 131–143. doi:10.1016/j.epsl.2012.08.037

301 Hervé, G., Schnepf, E., Chauvin, A., Lanos, P., Nowaczyk, N., 2011. Archaeomagnetic
 302 results on three Early Iron Age salt-kilns from Moyenvic (France). *Geophys. J. Int.* 185,
 303 144–156. doi:10.1111/j.1365-246X.2011.04933.x

304 Hervé, G., Chauvin, A., Lanos, P., 2013a. Geomagnetic field variations in Western Europe
 305 from 1500BC to 200AD. Part I: Directional secular variation curve. *Phys. Earth Planet.*
 306 *Inter.* 218, 1–13. doi:10.1016/j.pepi.2013.02.002

307 Hervé, G., Chauvin, A., Lanos, P., 2013b. Geomagnetic field variations in Western Europe
308 from 1500 BC to 200 AD. Part II: New intensity secular variation curve. *Phys. Earth*
309 *Planet. Inter.* 218, 51–65. doi:10.1016/j.pepi.2013.02.003

310 Hill, M.J., Lanos, P., Denti, M., Dufresne, P., 2008. Archaeomagnetic investigation of bricks
311 from the VIIIth–VIIth century BC Greek–indigenous site of Incoronata (Metaponto,
312 Italy). *Phys. Chem. Earth, Parts A/B/C* 33, 523–533. doi:10.1016/j.pce.2008.02.026

313 Hong, H., Yu, Y., Lee, C.H., Kim, R.H., Park, J., Doh, S.-J., Kim, W., Sung, H., 2013.
314 Globally strong geomagnetic field intensity circa 3000 years ago. *Earth Planet. Sci. Lett.*
315 383, 142–152. doi:10.1016/j.epsl.2013.09.043

316 Kapper, K.L., Donadini, F., Hirt, A.M., 2015. Holocene archeointensities from mid European
317 ceramics, slags, burned sediments and cherts. *Phys. Earth Planet. Inter.* 241, 21–36.
318 doi:10.1016/j.pepi.2014.12.006

319 Kovacheva, M., Boyadzhiev, Y., Kostadinova-Avramova, M., Jordanova, N., 2009. Updated
320 archeomagnetic data set of the past eight millenia from the Sofia laboratory, Bulgaria.
321 *Geochemistry Geophys. Geosystems* 10. doi:10.1029/2008GC002347

322 Kovacheva, M., Kostadinova-Avramova, M., Jordanova, N., Lanos, P., Boyadzhiev, Y., 2014.
323 Extended and revised archaeomagnetic database and secular variation curves from
324 Bulgaria for the last eight millennia. *Phys. Earth Planet. Inter.* 236, 79–94.
325 doi:10.1016/j.pepi.2014.07.002

326 Ledger, P., Miras, Y., Poux, M., Milcent, P.-Y. 2015. The Palaeoenvironmental Impact of
327 Prehistoric Settlement and Proto-Historic Urbanism: Tracing the Emergence of the

328 Oppidum of Corent, Auvergne, France. *PLoS ONE*, 10(4): e0121517.
 329 doi:10.1371/journal.pone.0121517.

330 Milcent, P.-Y., Poux, M., Mader, S., Torres, M., Tramon, A., 2014a. Une agglomération de
 331 hauteur autour de 600 a.C. en Gaule centrale : Corent (Auvergne). *In* : Alberti G., Féliu
 332 Cl., Pierrevelcin G. (eds.) *Transalpinare. Mélanges offerts à Anne-Marie Adam*,
 333 Ausonius Editions, Collection Mémoires, 36, Bordeaux, 2014, 181-204.

334 Milcent, P.-Y., Chassan, N., Mader, S., Saint-Sever, G., Tramon, A., 2014b. Les occupations
 335 de l'âge du Bronze du plateau de Corent (Auvergne, Puy-de-Dôme) : résultats des
 336 campagnes de fouille 2010-2013. *Bull. de l'APRAB*, 12, 89-94.

337 Moutmir, A., 1995. Analyses magnétiques de terres cuites protohistoriques en France.
 338 Apports en archéomagnétisme (Premier millénaire avant J.-C.) et en archéologie.
 339 Muséum National d'histoire Naturelle, Paris.

340 Pavón-Carrasco, F.J., Osete, M.L., Torta, J.M., De Santis, A., 2014a. A geomagnetic field
 341 model for the Holocene based on archaeomagnetic and lava flow data, *Earth Planet. Sci.*
 342 *Lett.* 388, 98-109.

343 Pavón-Carrasco, F.J., Gomez-Paccard, M., Hervé, G., Osete, M.L., Chauvin, A., 2014b.
 344 Intensity of the geomagnetic field in Europe for the last 3 ka: Influence of data quality on
 345 geomagnetic field modeling. *Geochemistry Geophys. Geosystems* 1–16.
 346 doi:10.1002/2014GC005311

347 Prévot, M., Mankinen, E.A., Coe, R.S., Grommé, C.S., 1985. The Steens Mountain (Oregon)
 348 geomagnetic polarity transition, 2. Field intensity variations and discussion of reversal
 349 models. *J. Geophys. Res.* 90, 10417–10448.

350 Schnepf, E., Lanos, P., Chauvin, A., 2009. Geomagnetic paleointensity between 1300 and
 351 1750 A.D. derived from a bread oven floor sequence in Lübeck, Germany.
 352 *Geochemistry, Geophys. Geosystems* 10, doi:10.1029/2009GC002470

353 Shaar, R., Ben-Yosef, E., Ron, H., Tauxe, L., Agnon, A., Kessel, R., 2011. Geomagnetic field
 354 intensity: How high can it get? How fast can it change? Constraints from Iron Age
 355 copper slag. *Earth Planet. Sci. Lett.* 301, 297–306. doi:10.1016/j.epsl.2010.11.013

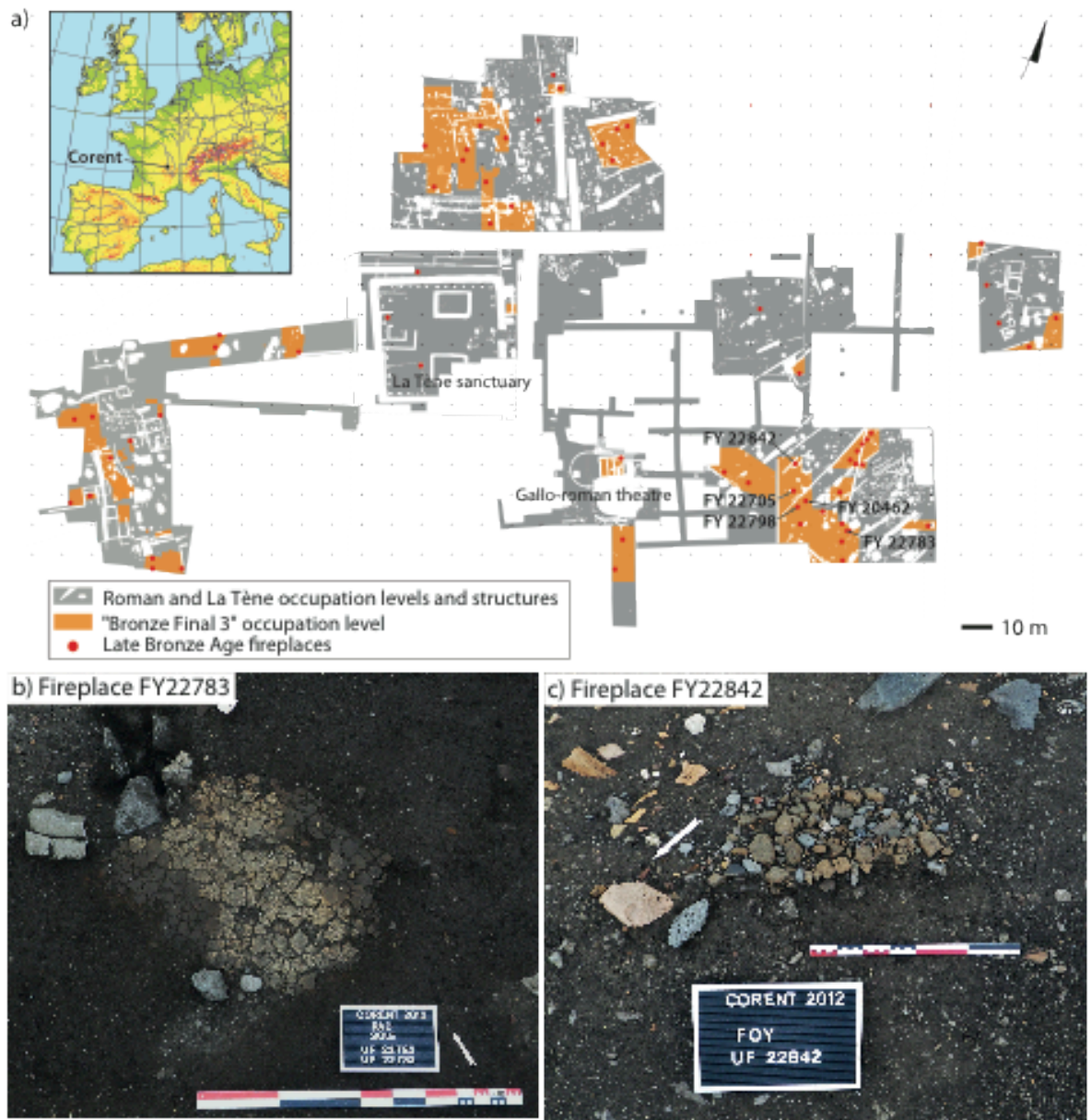
356 Tema, E., Morales, J., Goguitchaichvili, A., Camps, P., 2013. New archaeointensity data from
 357 Italy and geomagnetic field intensity variation in the Italian Peninsula. *Geophys. J. Int.*
 358 193, 603–614. doi:10.1093/gji/ggs120

359 Thellier, E., Thellier, O., 1959. Sur l'intensité du champ magnétique terrestre dans le passé
 360 historique et géologique. *Ann. Géophysique* 15, 285–376.

361
 362

363

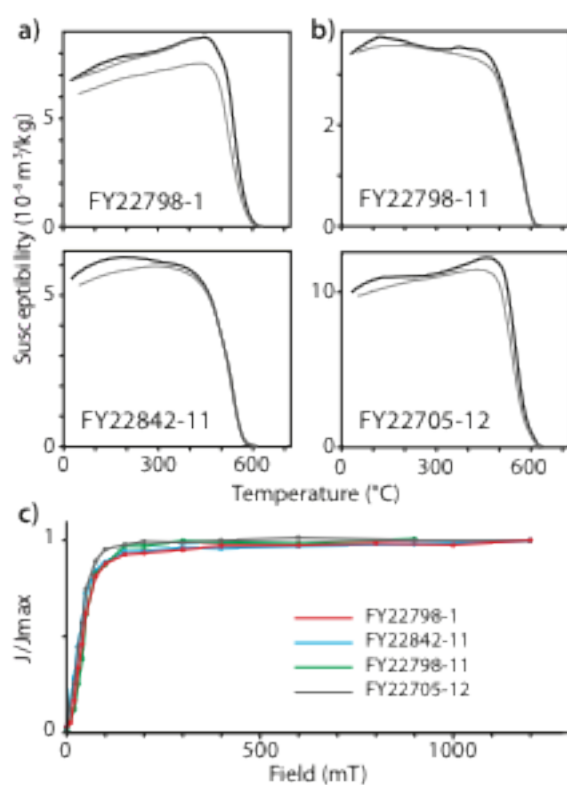
364 Figure 1: Map of the central area of Corent archaeological site (2001 to 2015
365 excavations) emphasizing the levels from the Late Bronze Age (“Bronze Final 3”) and
366 their associated fireplaces (a) and pictures of two sampled fireplaces (b-c).



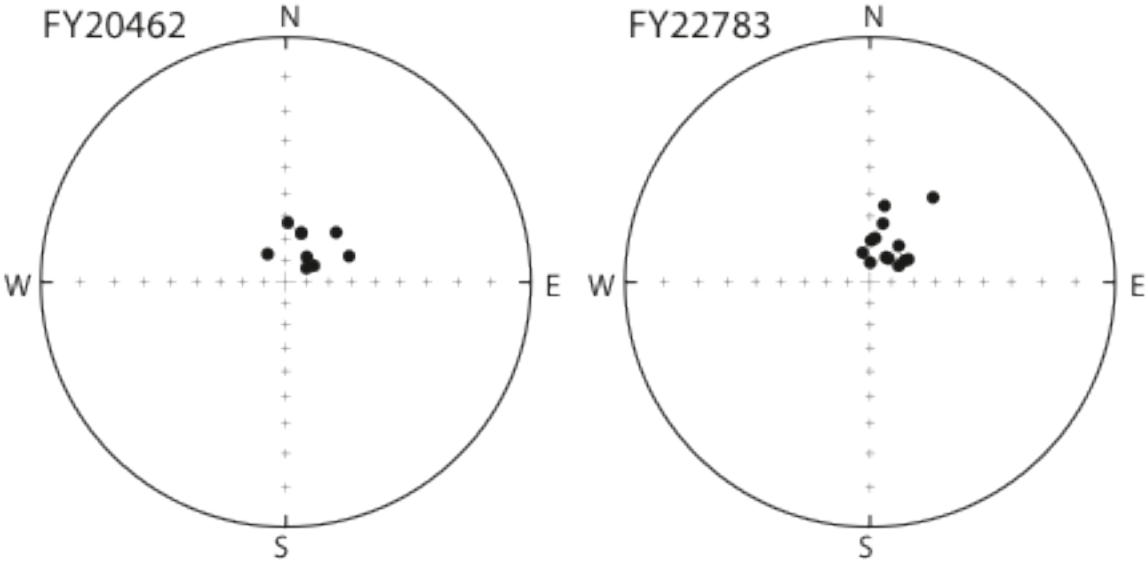
367

368

Figure 2: Representative magnetic mineralogy results with thermomagnetic curves of baked clay fragments (a) and of pottery sherds (b) together with acquisition curves of isothermal remanent magnetization (c). In thermomagnetic curves, the black curve is the variation of susceptibility during the heating and the grey curve during the cooling.



375 Figure 3: Stereographic plot of the TRM directions obtained on oriented block samples
376 from FY20462 and FY22783 fireplaces.



377

378

Figure 4: Archaeointensity results of baked clay fragments (a-b) and of pottery sherds (c). Solid circles on NRM-TRM diagrams indicate the temperature steps used in the intensity determination. Corresponding demagnetization directions are shown in sample coordinates in the orthogonal diagrams. Open (solid) circles denote the projection on the vertical (horizontal) plane.

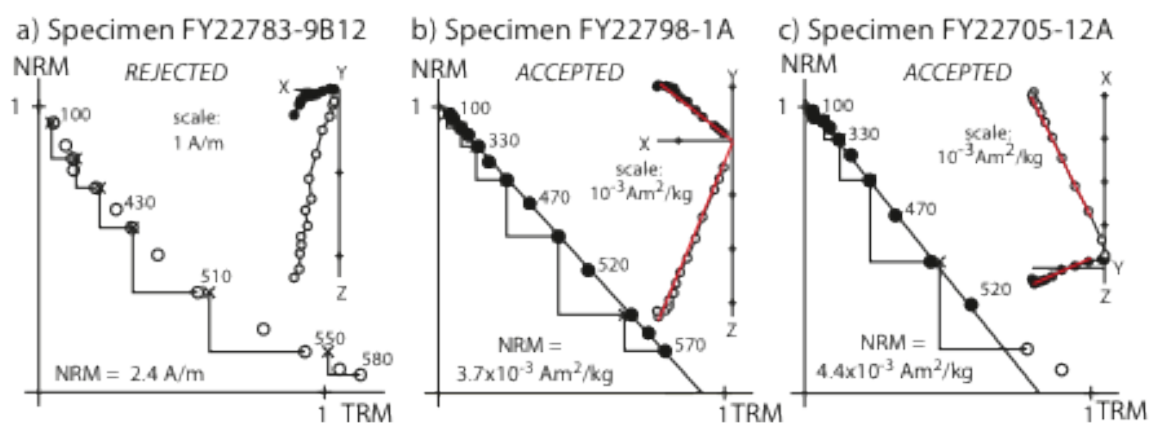


Figure 5: Secular variation of the geomagnetic intensity at the Late Bronze and Iron Ages in Western Europe. Corent data (red squares) are plotted with other published data (black squares represent the selection of Hervé et al. 2013b, whereas gray circles and triangles are the Swiss data of Kapper et al. 2015). The gray triangle indicates the Swiss data with an unusual standard deviation discussed in the text. All data are relocated to Paris. The blue curve is the mean intensity with its 95 per cent confidence envelop predicted by the geomagnetic model SHA.DIF.14k (Pavón-Carrasco et al., 2014). The Swiss data in grey are not included in this model.

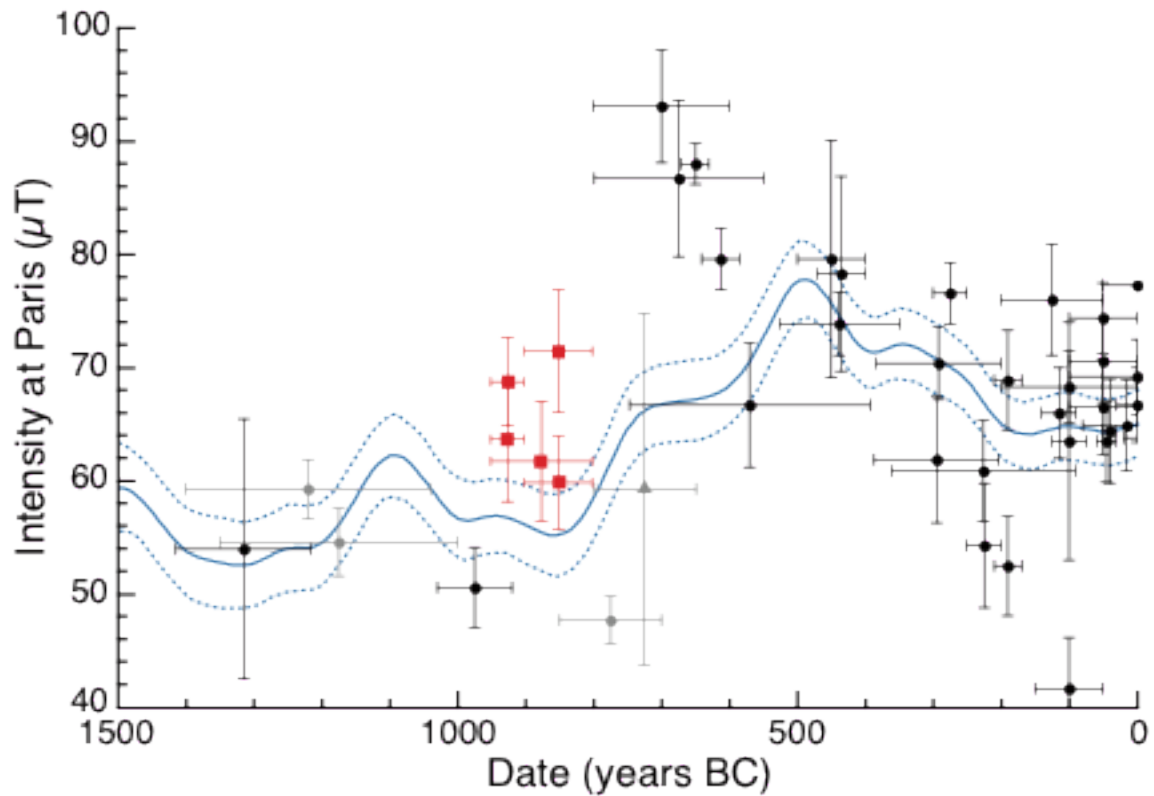


Table 1: Archaeological dating and mean archaeointensities of studied fireplaces. Fireplace, name of the sampled structure; Age, dating interval in years BC of the last use of the fireplace; N, number of specimens used in the calculation of the structure mean archaeointensity; $F \pm SD$, mean raw archaeointensity and standard deviation; $F_a \pm SD$, mean archaeointensity and standard deviation corrected for TRM anisotropy; $F_{a+c} \pm SD$, mean archaeointensity and standard deviation corrected for TRM anisotropy and cooling rate; F_{Paris} , mean archaeointensity relocated to Paris using Virtual Axial Dipole Moment correction.

Fireplace	Age (BC)	N	$F \pm SD$ (μT)	$F_a \pm SD$ (μT)	$F_{a+c} \pm SD$ (μT)	F_{Paris} (μT)
FY20462	[950; 900]	8	69.7 ± 5.6	70.3 ± 5.7	61.6 ± 5.5	63.6
FY22783	[950; 900]	12	65.2 ± 3.1	69.0 ± 3.8	66.5 ± 3.9	68.7
FY22798	[900; 800]	6	62.5 ± 5.5	60.7 ± 4.0	57.9 ± 4.1	59.8
FY22705	[900; 800]	12	71.5 ± 4.5	71.6 ± 4.8	69.2 ± 5.4	71.4
FY22842	[950; 800]	10	60.5 ± 4.8	60.8 ± 5.0	59.7 ± 5.3	61.7